ChemComm

COMMUNICATION

Electric-field effects on the [FeFe]-hydrogenase active site†

Arndt R. Finkelmann, Martin T. Stiebritz and Markus Reiher*

The effect of a homogeneous electric field—as exerted by the protein environment and by an electrode potential—on the reactivity of the active site of [FeFe] hydrogenases is unravelled by density functional theory calculations.

Hydrogenases have been applied in electrochemical processes to produce molecular dihydrogen for clean-energy technologies.[1] Electric fields affect the electronic structure and thus the reactivity of the active site. It is known that [NiFe] hydrogenases adsorbed on electrodes experience dispersion of reaction rates.[2] This can be attributed to different orientations at the electron-transfer interface, though other effects, like double-layer potentials, might also be important.[2,3] In general, little is known about the details of the interaction of stable and reactive intermediates with external fields in such situations. Here, we systematically investigate to what extent such fields can modify the energetics of key reaction steps at the active site of [FeFe] hydrogenases, which is the most desirable candidate for dihydrogen production. We should note that studies in a similar spirit have been performed for cytochrome P450 and proton transfer in a DNA base pair.[4]

[FeFe] hydrogenases catalyze the reversible formation of H_2 with a high turnover frequency.[5] The active site, the H-cluster, consists of a [4Fe–4S] cubane linked *via* a cysteine bridge to the so called $[2Fe]_H$ subcluster. The latter comprises two iron atoms, one proximal (Fe_p) and one distal (Fe_d) to the cubane, and an azadithiolate bridging ligand.[6] H_2 formation at the H-cluster comprises proton/electron transfer steps and proceeds *via* a H^- species terminally bound to Fe_d.[7,8] A crucial decomposition reaction, which one seeks to avoid, is the O_2-induced inhibition that initiates the degradation of the enzyme starting with O_2 coordination to Fe_d.[9]

Chemical processes at active sites of such metalloproteins are usually well described by a quantum mechanical (QM) model that considers only the active site and some important amino acid residues.[10] While the electric field of a surrounding protein may be approximated by a polarizable dielectric continuum model in a sufficiently large QM model, the strength of electric fields exerted on proteins adsorbed on polarized electrodes is difficult to assess.[11]

In order to systematically screen electric-field effects on our 96-atom QM model (Fig. 1, left), we first need to understand the magnitude and direction of the field exerted by the protein itself on the active site. We extract this information from the electrostatic potential that we obtain by numerical solution of the Poisson–Boltzmann equation for the crystal structure of [FeFe] hydrogenase from *Clostridium pasteurianum* (pdb code: 3C8Y) and from *Desulfovibrio desulfuricans* (pdb code: 1HFE) (detailed information can be found in the ESI†).[12] The field within a protein is then obtained as the derivative of the electrostatic potential at the position of interest; in our case at the position of the Fe_d atom. The resulting local field vectors at Fe_d, $\vec{E}^0_{prot}(\vec{r}_{Fe_d})$, are shown in Fig. 1 (red vectors) and were found to have a length of 0.0038 for *C. pasteurianum* and of 0.0026 for *D. desulfuricans*, both measured in Hartree atomic units (a.u.), in which the elementary charge and $4\pi\varepsilon_0$ assume a value of one. Remarkably, these two field strengths are very
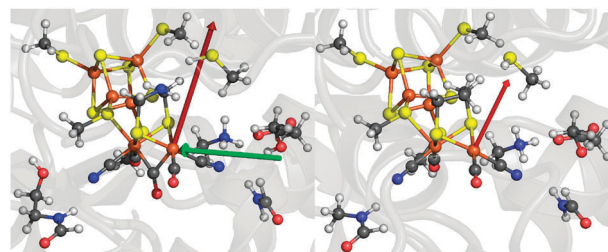

Fig. 1 Left: 96-atom QM model of the active site extracted from *Clostridium pasteurianum* (pdb code: 3C8Y). The red arrow represents the effective field vector of the protein surrounding at Fe_d ($\vec{E}^0_{prot}$) and the green arrow indicates the arbitrarily chosen external field along the Fe–Fe bond ($\vec{E}_{Fe–Fe}$). Right: corresponding presentation for *Desulfovibrio desulfuricans* (pdb code: 1HFE), where the red arrow again represents the effective field at Fe_d. Color code: C, grey; Fe, brown; H, white; N, blue; O, red; S, yellow.

ETH Zürich, Laboratorium für Physikalische Chemie, Wolfgang-Pauli-Strasse 10, 8093 Zürich, Switzerland. E-mail: markus.reiher@phys.chem.ethz.ch; Fax: +41 446331594; Tel: +41 446334308
† Electronic supplementary information (ESI) available: Computational details, additional tables and structures. See DOI: 10.1039/c3cc44112a
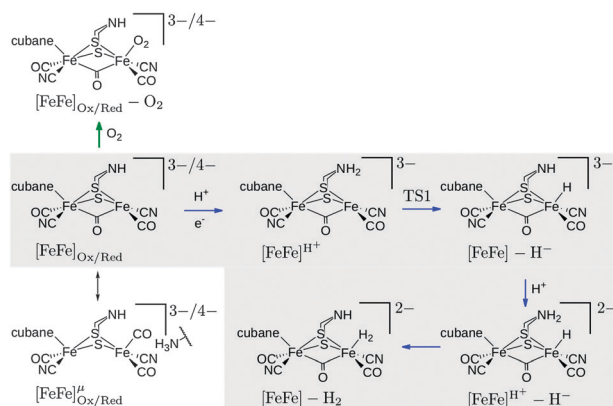
Communication

Fig. 2 Investigated intermediates and reactions. The reactions in the grey box correspond to reaction steps of the catalytic cycle (blue arrows). O_2 addition is indicated by a green arrow. The oxidized state corresponds to the formal oxidation state $Fe_p(II)Fe_d(I)$, the reduced state to $Fe_p(I)Fe_d(I)$. The oxidized species are doublets ($S = 1/2$), all other species are singlets ($S = 0$). Note that the Lewis structures shown do not represent the full QM model (cf. Fig. 1). The charge given is the charge of the full QM model.

similar and they also point in almost the same direction (see Fig. 1), although the sequence identity of the two enzymes is only 30%. Based on this information, a homogeneous electric field, $\vec{E}_{prot}^{0}(\vec{r}) = \vec{E}_{prot}^{0}(\vec{r}_{Fe_d})$, was derived to enter into the Kohn–Sham equations in the BP86-D3/def2-TZVP calculations on the 96-atom QM model of *C. pasteurianum* (see ESI† for details).

The external field in an electrochemical experiment would be screened by the protein and water surroundings of the H-cluster. Thus, in a sequence of calculations the field strength was varied in steps of ± 0.001, ± 0.002, ± 0.003 a.u. around the reference of 0.0038 a.u. (denoted $\vec{E}_{prot}^{\pm 1}$, $\vec{E}_{prot}^{\pm 2}$ and $\vec{E}_{prot}^{\pm 3}$) in order to investigate a possible external-field effect. In a second set of calculations, a field pointing from Fe_p to Fe_d, $\vec{E}_{Fe-Fe}$, with a fixed strength of 0.0038 a.u. was applied to investigate the effect of a change in the field direction. $\vec{E}_{Fe-Fe}$, which is perpendicular to the plane that separates the $[2Fe]_H$ subcluster and the cubane, is particularly interesting as it can induce charge transfer between both parts. Finally, calculations were performed with inverted field directions, denoted by a minus sign, i.e., $-\vec{E}$. Reactants (including barriers) investigated with respect to field effects are depicted in Fig. 2.

The change in partial charges on individual atoms induced by the electric field is small and discussed in the ESI.† A clear trend is only revealed when the partial charges of the $[2Fe]_H$ subcluster and the cubane (including sulphur atoms of coordinating cysteines) are separately added up. For all intermediates the field in the direction of $\vec{E}_{prot}^{0}$ induces a shift of electron density from the cubane to the $[2Fe]_H$ subcluster. The negative charge on the cubane decreases by +0.09e to +0.17e for different intermediates (and the strongest field $\vec{E}_{prot}^{+3}$). The negative charge on the $[2Fe]_H$ subcluster increases by −0.05e to −0.13e, accordingly. The decrease in negative charge on the cubane is always smaller than the increase in negative charge on the $[2Fe]_H$ subcluster because the charge is shifted to the amino acid environment of the $[2Fe]_H$ subcluster. $\vec{E}_{Fe-Fe}$ induces a transfer of negative charge from the cubane to the $[2Fe]_H$ subcluster. Inversion of the field direction leads to the expected inversion of the charge shifts. Hence, the protein field clearly polarizes the active site towards the $[2Fe]_H$ subcluster. The inverse field has a less pronounced effect. The polarization could be enhanced by a field in the $\vec{E}_{Fe-Fe}$ direction (or lowered by $-\vec{E}_{Fe-Fe}$). The cubane serves as a charge reservoir and $\vec{E}_{Fe-Fe}$ and $\vec{E}_{prot}^{0}$ increase charge donation from the cubane and to the $[2Fe]_H$ subcluster.

The effect of the field on reaction energies of reaction steps in Fig. 2 of the catalytic cycle[8,13] are summarized in Table 1 (see ESI† for data of inverted fields). In reaction $[FeFe]^{H+} \rightarrow TS1 \rightarrow [FeFe] - H^-$ (rows 1–3 in Table 1) a proton is transferred from the bridgehead amine group to Fe_d to form the terminal hydride species. This reaction becomes less exothermic with increasing field in $\vec{E}$ strength. For $\vec{E}_{prot}^{+3}$ it is +10.7 kcal mol^{-1} less exothermic than in the field-free case. The reaction energy changes linearly with the field. For each increase in field strength the reaction becomes +1.6 kcal mol^{-1} less exothermic. By contrast, $\vec{E}_{Fe-Fe}$ leads to a −4.9 kcal mol^{-1} more exothermic reaction. For a less exothermic reaction the barrier is higher, while it is lower for a more exothermic reaction, but the change in barrier height is smaller than the change in reaction energy. The effect of $\vec{E}_{prot}^{0}$, $\vec{E}_{prot}^{\pm 3}$ and $-\vec{E}_{prot}^{0}$ on the energy profile of the reaction $[FeFe]^{H+} \rightarrow TS1 \rightarrow [FeFe] - H^-$ (terminal hydride formation) is shown in Fig. 3. For the H_2 formation reaction, $[FeFe]^{H+} - H^- \rightarrow [FeFe] - H_2$, the reaction is up to +4.3 kcal mol^{-1} less exothermic with increasing field in $\vec{E}_{prot}$ direction. This decrease

Table 1 Reaction energies in kcal mol^{-1} for the different electric field strengths calculated with BP86-D3/def2-TZVP (single-points on BP86-D3/in vacuo structures; no dielectric continuum model applied). The field strengths in a.u. are: $|\vec{E}_{prot}^{-3}| = 0.0008$, $|\vec{E}_{prot}^{-2}| = 0.0018$, $|\vec{E}_{prot}^{-1}| = 0.0028$, $|\vec{E}_{prot}^{0}| = 0.0038$, $|\vec{E}_{prot}^{+1}| = 0.0048$, $|\vec{E}_{prot}^{+2}| = 0.0058$, $|\vec{E}_{prot}^{+3}| = 0.0068$, $|\vec{E}_{Fe-Fe}| = |-\vec{E}_{Fe-Fe}| = 0.0038$

Intermediate	No field	$\vec{E}_{prot}^{-3}$	$\vec{E}_{prot}^{-2}$	$\vec{E}_{prot}^{-1}$	$\vec{E}_{prot}^{0}$	$\vec{E}_{prot}^{+1}$	$\vec{E}_{prot}^{+2}$	$\vec{E}_{prot}^{+3}$	$\vec{E}_{Fe-Fe}$	$-\vec{E}_{Fe-Fe}$
H_2 formation										
$[FeFe]^{H+} \xrightarrow{TSI} [H] - H^-$	−20.7	−19.5	−17.9	−16.3	−14.8	−13.2	−11.6	−10.0	−25.6	−17.5
$[FeFe]^{H+} \rightarrow TS1$	4.0	4.0	4.4	4.7	5.1	5.5	5.8	6.2	3.4	4.2
$[FeFe]^{H+} - H^- \rightarrow [FeFe] - H_2$	−6.4	−5.8	−5.2	−4.6	−4.0	−3.4	−2.8	−2.1	−0.9	−2.4
O_2 additions										
$[FeFe]_{Ox} \rightarrow [FeFe]_{Ox} - O_2$	−23.6	−23.4	−22.9	−22.2	−21.6	−21.0	−20.3	−19.6	−19.7	−27.2
$[FeFe]_{Red} \rightarrow [FeFe]_{Red} - O_2$	−17.2	−16.8	−16.3	−15.8	−15.3	−14.8	−14.3	−13.8	−15.6	−20.3
Reduction										
$[FeFe]_{Ox} \rightarrow [FeFe]_{Red}$	70.0	45.5	14.9	−15.8	−46.4	−77.0	−107.6	−138.2	62.8	78.4
$[FeFe]_{Ox}^{\mu} \rightarrow [FeFe]_{Red}^{\mu}$	77.9	53.5	22.4	−8.6	−39.6	−70.7	−101.7	−132.8	73.7	83.5

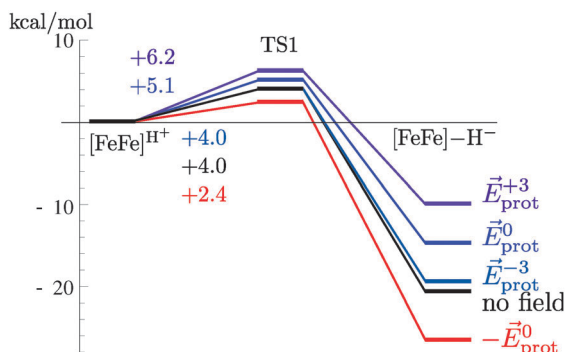**Fig. 3** Energy profiles for the reaction $[FeFe]^{H+} \rightarrow TS1 \rightarrow [FeFe] - H^-$ for different field strengths. The barriers are given in kcal mol^{-1}.

in exothermicity is linear as well. Importantly, both fields, $\vec{E}_{Fe-Fe}$ and $-\vec{E}_{Fe-Fe}$, lead to a decreased exothermicity (+5.5 and +4.0 kcal mol^{-1}, resp.) for H_2 formation. Hence, $\vec{E}_{prot}^0$ disfavors both proton transfer reactions, while $\vec{E}_{Fe-Fe}$ favors hydride transfer but disfavors H_2 formation.

The reduction of the H_2-coordinated species and the species with a free coordination site in the μ-bridging position are, of course, most affected by the electric field (last two rows in Table 1). Surprisingly, $\vec{E}_{Fe-Fe}$ has only a small effect on the energies. Moreover, with $\vec{E}_{prot}^{+3}$, the O_2 coordination energies become +4.0 and +3.4 kcal mol^{-1} less exothermic for the oxidized and reduced oxidation states, respectively, although the coordination reaction remains strongly exothermic.

To conclude, the polarization of the H-cluster induced by $\vec{E}_{Fe-Fe}$ is stronger than that induced by $\vec{E}_{prot}^0$. Inversion of both fields leads to inversion of differential polarization but with smaller magnitude. This is due to the excess of charge on the cubane in most intermediates. $\vec{E}_{prot}^0$ leads to a reduced exothermicity of hydride and H_2 formation which could be beneficial for the enzyme to work close to the thermodynamic equilibrium. Our results explicitly show that no crucial field-induced modulations of barrier heights and reaction energies are observed. The reversibility of the whole H_2 formation cycle is not affected. Still, we might speculate that the [FeFe] hydrogenase from *C. pasteurianum* should feature an activation pattern that favors H_2 oxidation and disfavors H_2 formation compared to the one from *D. desulfuricans* because the former exerts a stronger field at the ligand-binding site. The measured activity data appear to indicate such a trend for H_2 evolution.[14]

References

1 K. A. Vincent, A. Parker and F. A. Armstrong, *Chem. Rev.*, 2007, **107**, 4366–4413.
2 C. Léger, A. K. Jones, S. P. J. Albracht and F. A. Armstrong, *J. Phys. Chem. B*, 2002, **106**, 13058–13063.
3 J. Hirst and F. A. Armstrong, *Anal. Chem.*, 1998, **70**, 5062–5071.
4 S. Shaik, S. P. de Visser and D. Kumar, *J. Am. Chem. Soc.*, 2004, **126**, 11746–11749; J. P. Ceron-Carrasco and D. Jacquemin, *Phys. Chem. Chem. Phys.*, 2013, **15**, 4548–4553.
5 C. Madden, M. D. Vaughn, I. Díez-Pérez, K. A. Brown, P. W. King, D. Gust, A. L. Moore and T. A. Moore, *J. Am. Chem. Soc.*, 2012, **134**, 1577–1582.
6 J. C. Fontecilla-Camps, A. Volbeda, C. Cavazza and Y. Nicolet, *Chem. Rev.*, 2007, **107**, 4273–4303; A. Silakov, B. Wenk, E. Reijerse and W. Lubitz, *Phys. Chem. Chem. Phys.*, 2009, **11**, 6592–6599; G. Berggren, A. Adamska, C. Lambertz, T. R. Simmons, J. Esselborn, M. Atta, S. Gambarelli, J.-M. Mouseca, E. Reijerse, W. Lubitz, T. Happe, V. Artero and M. Fontecave, *Nature*, 2013, **499**, 66–69.
7 W. Lubitz, E. Reijerse and M. van Gastel, *Chem. Rev.*, 2007, **107**, 4331–4365; P. E. M. Siegbahn, J. W. Tye and M. B. Hall, *Chem. Rev.*, 2007, **107**, 4414–4435; D. W. Mulder, M. W. Ratzloff, E. M. Shepard, A. S. Byer, S. M. Noone, J. W. Peters, J. B. Broderick and P. W. King, *J. Am. Chem. Soc.*, 2013, **135**, 6921–6929; A. Adamska, A. Silakov, C. Lambertz, O. Rüdiger, T. Happe, E. Reijerse and W. Lubitz, *Angew. Chem., Int. Ed.*, 2012, **51**, 11458–11462.
8 H.-J. Fan and M. B. Hall, *J. Am. Chem. Soc.*, 2001, **123**, 3828–3829; Z.-P. Liu and P. Hu, *J. Chem. Phys.*, 2002, **117**, 8177–8180.
9 M. T. Stiebritz and M. Reiher, *Inorg. Chem.*, 2009, **48**, 7127–7140; M. T. Stiebritz and M. Reiher, *Inorg. Chem.*, 2010, **49**, 8645; S. T. Stripp, G. Goldet, C. Brandmayr, O. Sanganas, K. A. Vincent, M. Haumann, F. A. Armstrong and T. Happe, *Proc. Natl. Acad. Sci. U. S. A.*, 2009, **106**, 17331–17336; M. K. Bruska, M. T. Stiebritz and M. Reiher, *J. Am. Chem. Soc.*, 2011, **133**, 20588–20603; M. T. Stiebritz and M. Reiher, *Chem. Sci.*, 2012, **3**, 1739–1751; M. K. Bruska, M. T. Stiebritz and M. Reiher, *Dalton Trans.*, 2013, **42**, 8729–8735; M. Bergeler, M. T. Stiebritz and M. Reiher, *ChemPlusChem*, 2013, DOI: 10.1002/cplu.201300186.
10 P. E. M. Siegbahn and F. Himo, *Wiley Interdiscip. Rev.: Comput. Mol. Sci.*, 2011, **1**, 323–336; M. Podewitz, M. T. Stiebritz and M. Reiher, *Faraday Discuss.*, 2011, **148**, 119–135.
11 C. P. Smith and H. S. White, *Anal. Chem.*, 1992, **64**, 2398–2405; E. Gileadi, *Physical Electrochemistry: Fundamentals, Techniques and Applications*, Wiley-VCH, Weinheim, Germany, 2011.
12 A. S. Pandey, T. V. Harris, L. J. Giles, J. W. Peters and R. K. Szilagyi, *J. Am. Chem. Soc.*, 2008, **130**, 4533–4540; Y. Nicolet, C. Piras, P. Legrand, C. E. Hatchikian and J. C. Fontecilla-Camps, *Structure*, 1999, **7**, 13–23.
13 G. Zampella, C. Greco, P. Fantucci and L. De Gioia, *Inorg. Chem.*, 2006, **45**, 4109–4118; C. Greco, M. Bruschi, L. De Gioia and U. Ryde, *Inorg. Chem.*, 2007, **46**, 5911–5921; A. R. Finkelmann, M. T. Stiebritz, M. Reiher, 2013, submitted.
14 E. C. Hatchikian, N. Forget, V. M. Fernandez, R. Williams and R. Cammack, *Eur. J. Biochem.*, 1992, **209**, 357–365; M. W. Adams, *Biochim. Biophys. Acta*, 1990, **1020**, 115–145.